Electronic Supplementary Material (ESI) for Environmental Science: Atmospheres.

Supporting Material for: Multi-Day Photochemical Evolution of Organic Aerosol from Biomass Burning Emissions

Abraham Dearden[1], Yicong He[1,2,3], Ali Akherati[1,6], Christopher Y. Lim[4], Matthew M. Coggon[5], Abigail R. Koss[6], Joost de Gouw[7,8], Carsten Warneke[5], Lindsay D. Yee[9], John H. Seinfeld[10], Christopher D. Cappa[11], Jesse H. Kroll[4], Jeffrey R. Pierce[12], and Shantanu H. Jathar[1]

[1]Mechanical Engineering, Colorado State University, Fort Collins, CO, USA
[2]State Key Joint Laboratory of Environmental Simulation and Pollution Control, School of Environment, Tsinghua University, Beijing, China
[3]State Environmental Protection Key Laboratory of Sources and Control of Air Pollution Complex, Beijing, China
[4]Civil and Environmental Engineering, Massachusetts Institute of Technology, Cambridge, MA, USA
[5]Chemical Sciences Laboratory, National Oceanic and Atmospheric Administration, Boulder, CO, USA
[6]Tofwerk, Boulder, CO, USA
[7]Chemistry, University of Colorado Boulder, Boulder, CO, USA
[8]Cooperative Institute for Research in Environmental Sciences, Boulder, CO, USA
[9]Department of Environmental Science, Policy, and Management, Berkeley, CA, USA
[10]Department of Chemical Engineering, California Institute of Technology, Pasadena, CA, USA
[11]Civil and Environmental Engineering, University of California Davis, Davis, CA, USA
[12]Atmospheric Science, Colorado State University, Fort Collins, CO, USA
[*]Correspondence to: Shantanu H. Jathar (shantanu.jathar@colostate.edu)

Table S1: Summary of initial and final data for the 18 chamber experiments performed on 10 different fuels by Lim et al.[1] Experiments are ordered alphabetically by fuel.

Fire ID	***Fuel***	***Initial OA [µg m^{-3}]***	***Initial OA O:C***	***Initial SOA Precursors [ppbv]***	***Initial Seed Surface Area [µm^2 cm^{-3}]***	***Final OA [µg m^{-3}][&]***	***Final O:C***	***OH Exposure [molec. cm^{-3}]***	***Dilution Rate (hr^{-1})[#]***
62	Bear Grass	120	0.33	67	1.6×10^4	197	0.70	2.1×10^{11}	2.8
28	Chaparral #1	84	0.29	70	2.8×10^4	127	0.81	6.8×10^{11}	2.9
30	Chaparral #2	130	0.32	117	3.6×10^4	181	0.69	2.2×10^{11}	3.2
33	Chaparral #3	96	0.32	91	2.3×10^4	282	0.90	8.9×10^{11}	2.7
31	Douglas Fir #1	240	0.62	153	3.2×10^4	361	0.83	14×10^{11}	2.6
57	Douglas Fir #2	120	0.48	53	2.1×10^4	224	0.93	10×10^{11}	2.8
64	Douglas Fir #3	330	0.39	202	5.2×10^4	664	0.74	1.2×10^{11}	3.6
50	Dung	300	0.21	134	4.0×10^4	772	0.85	7.1×10^{11}	3.0
25	Engelmann Spruce #1	16	0.35	11	4.4×10^3	29	0.71	5.9×10^{11}	2.2
26	Engelmann Spruce #2	33	0.20	40	4.2×10^3	140	0.76	8.8×10^{11}	2.4
52	Engelmann Spruce #3	47	0.40	27	1.3×10^4	184	1.21	14×10^{11}	3.1
61	Excelsior	56	0.52	48	2.2×10^4	52	1.02	6.4×10^{11}	2.0
53	Loblolly Pine	66	0.35	52	1.2×10^4	161	0.96	5.3×10^{11}	2.8
21	Lodgepole Pine #1	48	0.25	15	6.6×10^3	80	0.74	6.8×10^{11}	2.1
41	Lodgepole Pine #2	23	0.38	12	2.7×10^3	92	1.28	8.2×10^{11}	2.1
38	Ponderosa Pine #1	29	0.36	18	8.2×10^3	58	0.92	8.6×10^{11}	2.4
39	Ponderosa Pine #2	240	0.31	123	3.0×10^4	392	0.76	3.4×10^{11}	2.9
56	Subalpine Fir	42	0.24	96	6.3×10^3	203	0.76	2.5×10^{11}	3.5
63[*]	Lodgepole Pine #3	180	0.37	85	4.6×10^4	110	0.64	N/A	3.3

[#]First-order dilution rate; [*]Dark experiment used to determine the bulk particle wall loss rate; [&]Corrected for particle wall losses

Table S2: VOC species measured by the PTR-ToF-MS and considered as SOA precursors in our model. Reproduced from the supporting information in Akherati et al.[2]

Species name	***Species Formula***	***k_{OH} [$cm^3\ s^{-1}\ molec.^{-1}$]***	***c^* [$\mu g\ m^{-3}$]***	***MW [$g\ mol^{-1}$]***	***Surrogate***
Pyrrole	C4H5N	1.45×10^{-10}	5.74×10^{7}	67.0892	Heterocyclics
Furan	C4H4O	4.00×10^{-11}	2.23×10^{9}	68.07356	Heterocyclics
Isoprene	C5H8	1.00×10^{-10}	2.05×10^{9}	68.11702	Biogenics
Dihydropyrrole	C4H7N	1.04×10^{-10}	5.15×10^{7}	69.10508	Heterocyclics
Tetrahydropyrrole	C4H9N	7.85×10^{-11}	2.44×10^{8}	71.12096	Heterocyclics
Benzene	C6H6	1.22×10^{-12}	4.05×10^{8}	78.11184	Aromatics
Pyridine	C5H5N	3.70×10^{-13}	5.28×10^{7}	79.0999	Heterocyclics
Methylpyrrole	C5H7N	1.10×10^{-10}	5.69×10^{7}	81.11578	Heterocyclics
MethylFuran	C5H6O	7.80×10^{-11}	7.71×10^{8}	82.10014	Heterocyclics
Thiophene	C4H4S	9.53×10^{-12}	3.64×10^{8}	84.13956	Heterocyclics
Furanone	C4H4O2	5.66×10^{-11}	1.34×10^{7}	84.07256	Heterocyclics
Ethynylpyrrole	C6H5N	6.45×10^{-11}	3.95×10^{6}	92.11854	Heterocyclics
Toluene	C7H8	5.63×10^{-12}	1.42×10^{8}	92.13842	Aromatics
2-Furancarbonitrile	C5H3NO	7.15×10^{-12}	1.81×10^{5}	93.08302	Heterocyclics
Methylpyridine	C6H7N	1.10×10^{-12}	4.36×10^{7}	93.12648	Heterocyclics
Phenol	C6H6O	2.80×10^{-11}	2.11×10^{6}	94.11084	Oxygenated Aromatics
4-pyridinol	C5H5NO	7.65×10^{-11}	1.81×10^{6}	95.0989	Heterocyclics
C2-pyrroles	C6H9N	2.00×10^{-10}	4.16×10^{6}	95.14236	Heterocyclics
Furfural	C5H4O2	3.56×10^{-11}	1.14×10^{7}	96.08326	Heterocyclics
Dimethylfuran	C6H8O	2.00×10^{-10}	1.40×10^{7}	96.12672	Heterocyclics
Methylthiophene	C5H6S	9.51×10^{-12}	1.28×10^{8}	98.16614	Heterocyclics
2-Methanolfuran	C5H6O2	1.04×10^{-10}	3.88×10^{6}	98.09914	Heterocyclics
Dihydrofurandione	C4H4O3	8.56×10^{-13}	9.00×10^{3}	100.0716	Heterocyclics
Phenylacetylene	C8H6	8.02×10^{-12}	2.16×10^{6}	102.1332	Aromatics
Benzonitrile	C7H5N	3.44×10^{-13}	4.62×10^{6}	103.1213	Aromatics
Styrene	C8H8	5.80×10^{-11}	3.43×10^{7}	104.1491	Aromatics
Vinylpyridine	C7H7N	2.66×10^{-11}	1.55×10^{6}	105.1372	Heterocyclics
Benzaldehyde	C7H6O	1.20×10^{-11}	7.30×10^{6}	106.1215	Aromatics
C8 aromatics	C8H10	1.32×10^{-11}	4.88×10^{7}	106.165	Aromatics
Pyridine aldehyde	C6H5NO	1.71×10^{-11}	7.85×10^{4}	107.1096	Heterocyclics
Dimethylpyridine	C7H9N	2.79×10^{-12}	2.05×10^{7}	107.1531	Heterocyclics
Benzoquinone	C6H4O2	4.51×10^{-12}	8.80×10^{5}	108.094	Aromatics
Cresol	C7H8O	5.30×10^{-11}	1.34×10^{7}	108.1374	Oxygenated Aromatics
Trimethylpyrrole	C7H11N	2.00×10^{-10}	1.20×10^{7}	109.1689	Heterocyclics
Benzenediol	C6H6O2	1.04×10^{-10}	1.10×10^{6}	110.1098	Oxygenated Aromatics
Trimethylfuran	C7H10O	1.59×10^{-10}	9.27×10^{7}	110.1533	Heterocyclics
Dihydroxypyridine	C5H5NO2	4.55×10^{-11}	3.78×10^{4}	111.0979	Heterocyclics
5-hydroxy 2-furfural	C5H4O3	4.90×10^{-11}	7.36×10^{5}	112.0823	Heterocyclics
Nitrofuran	C4H3NO3	5.06×10^{-12}	1.64×10^{4}	113.0703	Heterocyclics
5-hydroxymethyl-2[3H]-furanone	C5H6O3	1.00×10^{-10}	2.59×10^{5}	114.0981	Heterocyclics
5-hydroxy tetrahydro 2-furfural	C5H8O3	5.00×10^{-12}	7.36×10^{5}	116.114	Heterocyclics
Indene	C9H8	7.80×10^{-11}	1.06×10^{7}	116.1598	Aromatics

Benzeneacetonitrile	C8H7N	2.07×10^{-12}	5.72×10^{5}	117.1479	Aromatics
Benzofuran	C8H6O	3.70×10^{-11}	1.13×10^{7}	118.1322	Aromatics
Methylstyrene	C9H10	5.40×10^{-11}	1.14×10^{7}	118.1757	Aromatics
Isoindoline	C8H9N	8.00×10^{-11}	6.08×10^{5}	119.1638	Heterocyclics
Tolualdehyde	C8H8O	1.60×10^{-11}	2.39×10^{6}	120.1481	Aromatics
C9 aromatics	C9H12	2.20×10^{-11}	1.95×10^{7}	120.1916	Aromatics
Salicylaldehyde	C7H6O2	2.80×10^{-11}	3.72×10^{6}	122.1205	Aromatics
Dimethylphenol	C8H10O	5.05×10^{-11}	5.31×10^{6}	122.164	Oxygenated Aromatics
Nitrobenzene	C6H5NO2	1.40×10^{-13}	1.50×10^{6}	123.1086	Aromatics
Hydroxy benzoquinone	C6H4O3	1.30×10^{-11}	4.11×10^{5}	124.093	Aromatics
Guaiacol	C7H8O2	7.53×10^{-11}	9.16×10^{5}	124.1364	Oxygenated Aromatics
Hydroxymethylfurfural	C6H6O3	1.00×10^{-10}	4.11×10^{5}	126.1088	Heterocyclics
Dihydroxymethylfuran	C6H8O3	1.29×10^{-10}	4.11×10^{5}	128.1247	Heterocyclics
Naphthalene	C10H8	2.30×10^{-11}	5.73×10^{5}	128.1705	Aromatics
Dihydronaphthalene	C10H10	6.42×10^{-11}	5.11×10^{6}	130.1864	Aromatics
Methylindole	C9H9N	2.00×10^{-10}	3.64×10^{4}	131.1745	Aromatics
Methyl benzofuran	C9H8O	9.75×10^{-11}	3.54×10^{6}	132.1588	Heterocyclics
Methyl propenyl benzene	C10H12	3.30×10^{-11}	6.76×10^{6}	132.2023	Aromatics
3-methylacetophenone	C9H10O	2.42×10^{-12}	1.60×10^{6}	134.1747	Aromatics
C10 aromatics	C10H14	9.50×10^{-12}	1.04×10^{7}	134.2182	Aromatics
Methylbenzoicacid	C8H8O2	1.20×10^{-11}	1.66×10^{4}	136.1471	Aromatics
Monoterpenes	C10H16	1.63×10^{-10}	2.16×10^{7}	136.234	Biogenics
Nitrotoluene	C7H7NO2	7.72×10^{-13}	5.96×10^{5}	137.1352	Aromatics
MethylGuaiacol	C8H10O2	3.98×10^{-11}	5.62×10^{5}	138.163	Oxygenated Aromatics
Methylnaphthalene	C11H10	5.65×10^{-11}	5.20×10^{5}	142.1971	Aromatics
Naphthol	C10H8O	2.00×10^{-10}	2.71×10^{5}	144.1695	Aromatics
Ethylindene	C11H12	6.36×10^{-11}	1.67×10^{6}	144.213	Aromatics
Dimethylbenzofuran	C10H10O	1.20×10^{-10}	2.71×10^{5}	146.1854	Aromatics
Methylchavicol	C10H12O	5.43×10^{-11}	1.13×10^{6}	148.2013	Oxygenated Aromatics
C11 aromatics	C11H16	5.00×10^{-11}	4.81×10^{6}	148.2447	Aromatics
Vinyl guaiacol	C9H10O2	5.44×10^{-11}	2.28×10^{5}	150.1737	Oxygenated Aromatics
Vanillin	C8H8O3	2.73×10^{-11}	7.00×10^{5}	152.1461	Oxygenated Aromatics
Acenaphthylene	C12H8	7.55×10^{-11}	6.18×10^{4}	152.1919	Aromatics
Camphor	C10H16O	4.30×10^{-12}	1.98×10^{6}	152.233	Biogenics
Syringol	C8H10O3	9.66×10^{-11}	1.00×10^{5}	154.162	Oxygenated Aromatics
Cineole	C10H18O	2.26×10^{-11}	1.63×10^{7}	154.2489	Biogenics
1,3-dimethylnaphthalene	C12H12	6.94×10^{-11}	8.57×10^{4}	156.2237	Aromatics
Decanal	C10H20O	3.45×10^{-11}	1.27×10^{6}	156.2648	Alkanes
C12 aromatics	C12H18	1.13×10^{-10}	1.17×10^{6}	162.2713	Aromatics
Isoeugenol	C10H12O2	8.84×10^{-11}	1.94×10^{5}	188.2217	Oxygenated Aromatics
C13 aromatics	C13H20	1.13×10^{-10}	7.17×10^{5}	176.2979	Aromatics
Sesquiterpenes	C15H24	3.00×10^{-10}	4.58×10^{4}	204.3511	Biogenics
5-methyl furfural	C6H6O2	5.18×10^{-11}	1.10×10^{6}	110.1098	Heterocyclics

Table S3: SOM grids, surrogates, and parameters used in this work to perform the low NO_X simulations.

Precursor Class	***VOC Surrogate***	***ΔLVP***	m_{frag}	$p_{f,1}$	$p_{f,2}$	$p_{f,3}$	$p_{f,4}$	f_{HOM}	***Reference***
Benzene	benzene	2.081	0.001	0.122	0.019	0.709	0.151	0.002	Ng et al.[4]
Toluene	toluene	1.970	0.039	0.197	0.564	0.011	0.228	0.001	Zhang et al.[5]
C_{8+} single-ring aromatics	*m*-xylene	1.994	0.029	0.042	0.045	0.769	0.144	0.014	Ng et al.[4]
Polycyclic aromatic hydrocarbons (PAH)	naphthalene	1.946	0.029	0.012	0.498	0.480	0.010	0.018	Zhang et al.[5]
Isoprene	isoprene	1.624	0.107	0.426	0.002	0.558	0.015	0.000	Chhabra et al.[6]
Terpene	α-pinene	1.588	0.112	0.431	0.002	0.552	0.015	0.034	Chhabra et al.[6]
Oxygenated aromatics	phenol	1.977	0.404	0.067	0.096	0.823	0.014	0.001	Yee et al.[7]
Heterocyclic compounds	2-methylfuran, dimethylfuran	Same as high NO_X parameters from Table S4							He et al.[8]

Table S4: SOM grids, surrogates, and parameters used in this work to perform the high NO_X simulations.

Precursor Class	***VOC Surrogate***	***ΔLVP***	m_{frag}	$p_{f,1}$	$p_{f,2}$	$p_{f,3}$	$p_{f,4}$	***Reference***
Benzene	benzene	1.5495	0.7895	0.0743	0.0213	0.8963	0.0081	Ng et al.[4]
Toluene	toluene	1.4169	1.3064	0.5634	0.3413	0.0016	0.0937	Zhang et al.[5]
C_{8+} single-ring aromatics	*m*-xylene	1.4601	0.0736	0.1418	0.2971	0.4571	0.1040	Ng et al.[4]
Polycyclic aromatic hydrocarbons (PAH)	naphthalene	1.4922	0.7673	0.8138	0.0072	0.0635	0.1155	Zhang et al.[5]
Isoprene	isoprene	1.8742	0.5207	0.9924	0.0003	0.0065	0.0009	Chhabra et al.[6]
Terpene	α-pinene	1.9139	0.1312	0.5991	0.2923	0.1079	0.0007	Chhabra et al.[6]
Oxygenated aromatics	phenol, guaiacol	2.023	0.315	0.109	0.048	0.439	0.404	Yee et al.[7]
Oxygenated aromatics	syringol	1.629	0.148	0.394	0.121	0.071	0.414	Yee et al.[7]
Heterocyclic compound	2-methylfuran, dimethylfuran	1.459	0.449	0.0005	0.0014	0.998	0.0001	He et al.[8]

Table S5: VOC species measured by the PTR-ToF-MS and considered as additional SOA precursors in our model.

Species name	***Species Formula***	k_{OH} $[cm^3\ molecules^{-1}\ s^{-1}]$	***MW*** $[g\ mol^{-1}]$
Butenes	C4H8H	3.18×10^{-11}	56.1060
Nitromethane	CH3NO2H	2.00×10^{-14}	61.0392
CarbonicAcid	H2CO3H	5.63×10^{-12}	62.0300
13cyclopentadiene	C5H6H	9.20×10^{-11}	66.1000
MVK MACR CA	C4H6OH	2.48×10^{-11}	70.0894
Pentenemethylbutene	C5H10H	5.72×10^{-11}	70.1329
MEK	C4H8OH	5.46×10^{-12}	72.1053
Pentanenitriles	C5H9NH	5.00×10^{-13}	83.1317
3-methyl-3-buten-2-one	C5H8OH	1.15×10^{-11}	84.1000
Methylpropanoate	C4H8O2H	8.80×10^{-13}	88.1043
Pentacarbondioxide	C5O2H	4.60×10^{-10}	92.0500
4-methylpentanenitrile	C6H11NH	5.00×10^{-12}	97.2000
Methylcycpentanone/cyclohexanone	C6H10OH	6.40×10^{-12}	98.1426
Methylmethacrylate	C5H8O2H	3.03×10^{-11}	100.1150
Acetic anhydride	C4H6O3H	4.30×10^{-11}	102.0874
2-hydroxy-3-methyl-2-cycpenten-1-one	C6H8O2H	5.70×10^{-11}	112.0000
Ethylcyclopentanone	C7H12OH	1.00×10^{-11}	112.1692
Vinylethylacetate	C6H10O2H	2.00×10^{-11}	114.1416
Heptanal	C7H14OH	2.14×10^{-11}	114.1851
C6 esters	C6H12O2H	1.86×10^{-11}	116.1575

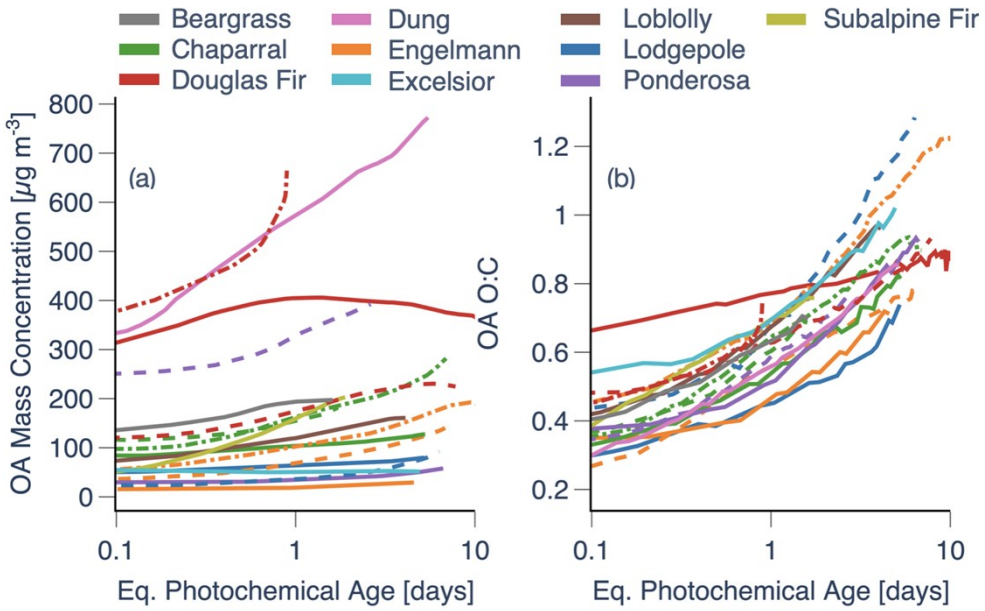

Figure S1: (a) Dilution and particle-wall-loss corrected measurements of OA mass concentration and (b) suspended OA O:C for the 18 chamber experiments studied in this work. Colors indicated different fuels. Different lines (solid, dashed, dash-dotted) with the same color are used to show experiments with the same fuel.

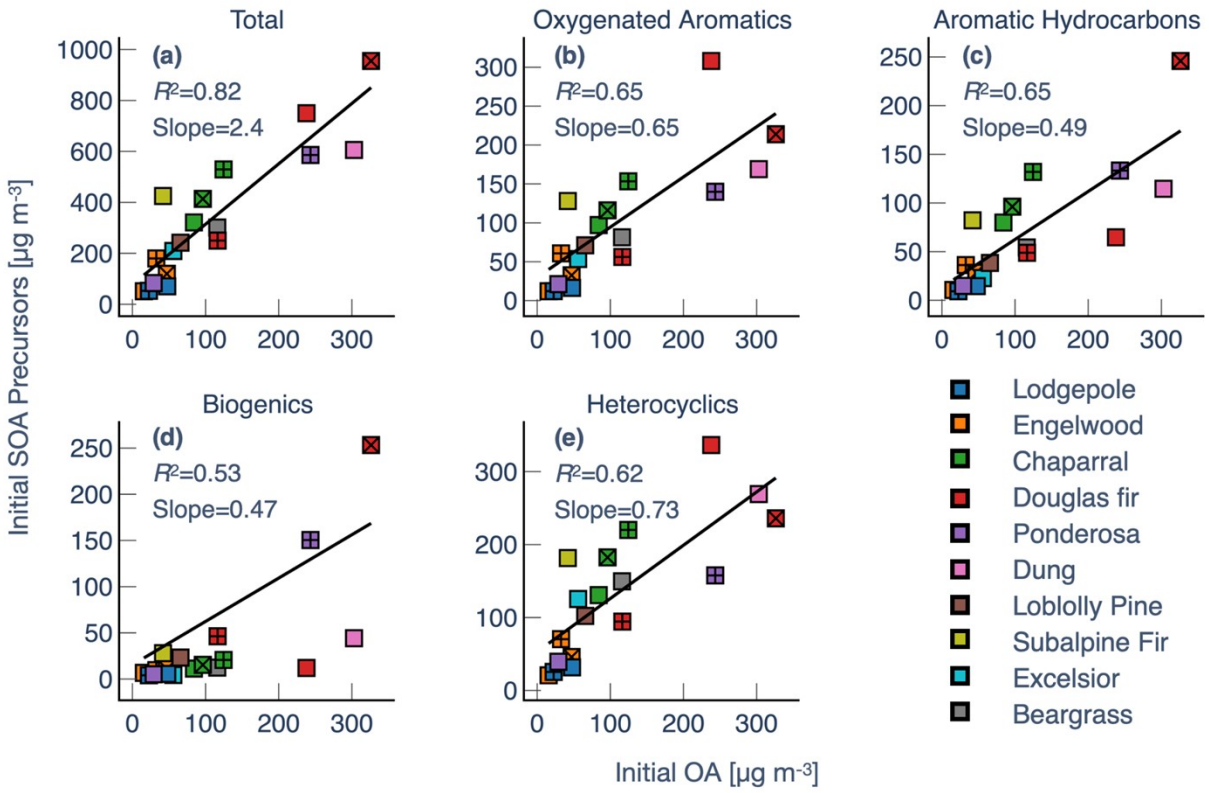

Figure S2: Initial precursor mass concentrations compared against initial OA mass concentrations for (a) all SOA precursors, (b) oxygenated aromatics, (c) aromatic hydrocarbons, (d) biogenic VOCs, and (e) heterocyclics. Data are presented for all 18 chamber experiments.

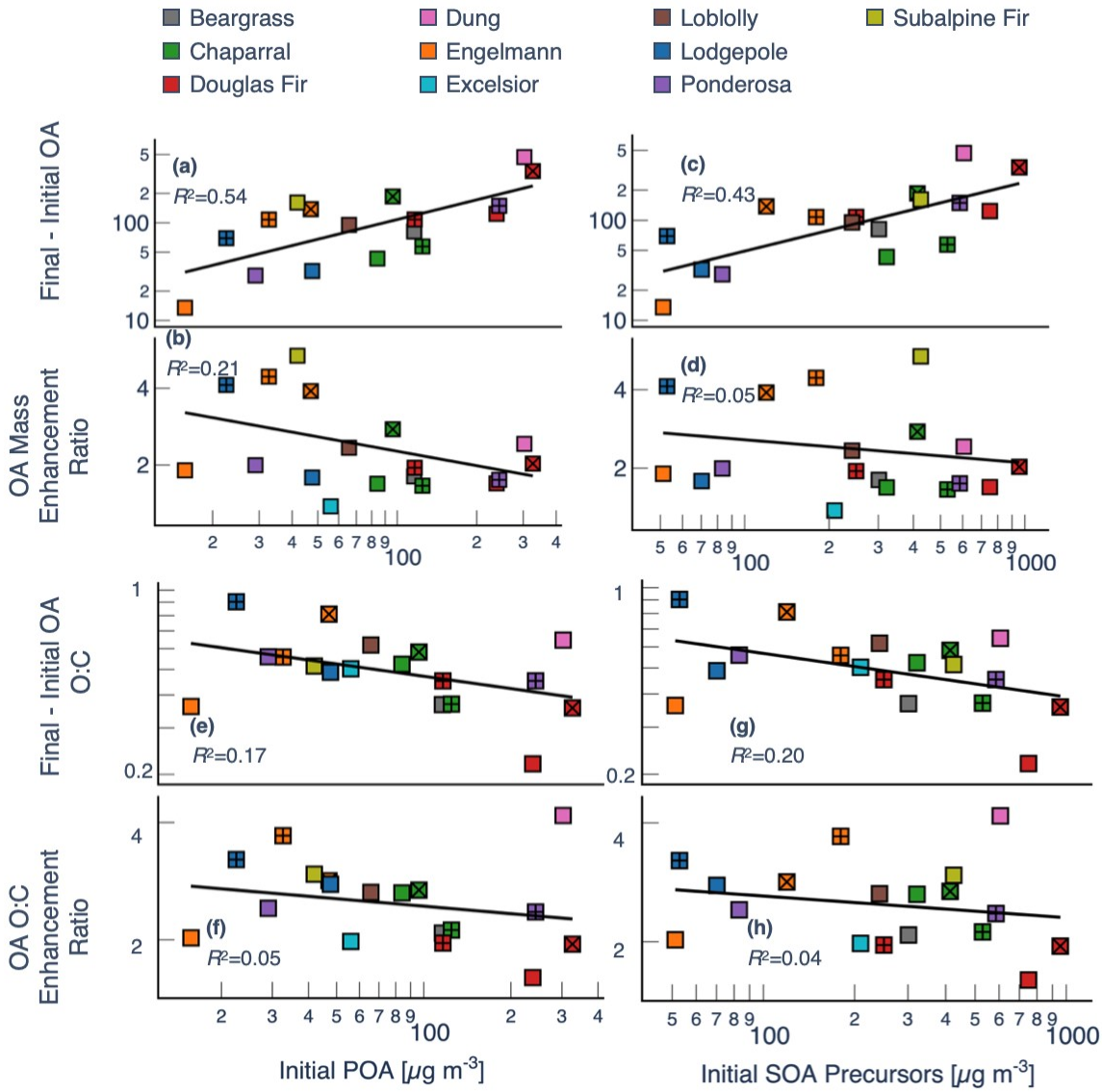

Figure S3: (a,c) OA added (dOA) and (b,d) OA mass enhancement ratio compared to (a,b) initial POA mass concentrations and (c,d) initial SOA precursor mass concentrations for all 18 chamber experiments. (e-h) represent the same for OA O:C. Trend lines are best fits to the data and are only meant to guide the eye.

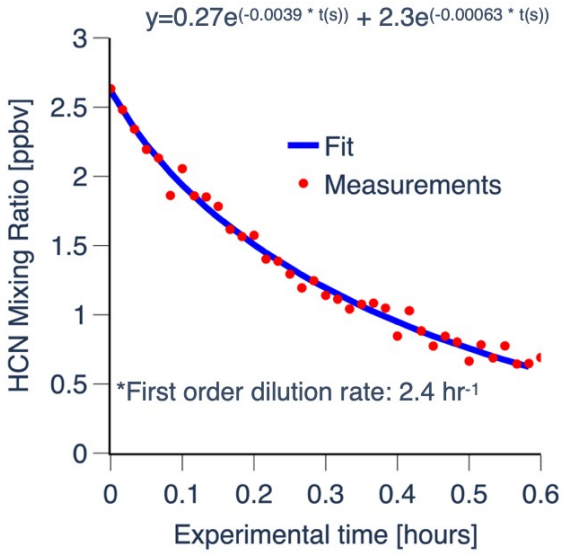

Figure S4: Measured hydrogen cyanide (HCN) mixing ratios and the double exponential fit where t is time in seconds used to calculate time-dependent dilution rates for the chamber experiment performed on Ponderosa Pine emissions (Fire 38). An interpretable first order dilution rate is also shown, calculated using a single exponential fit.

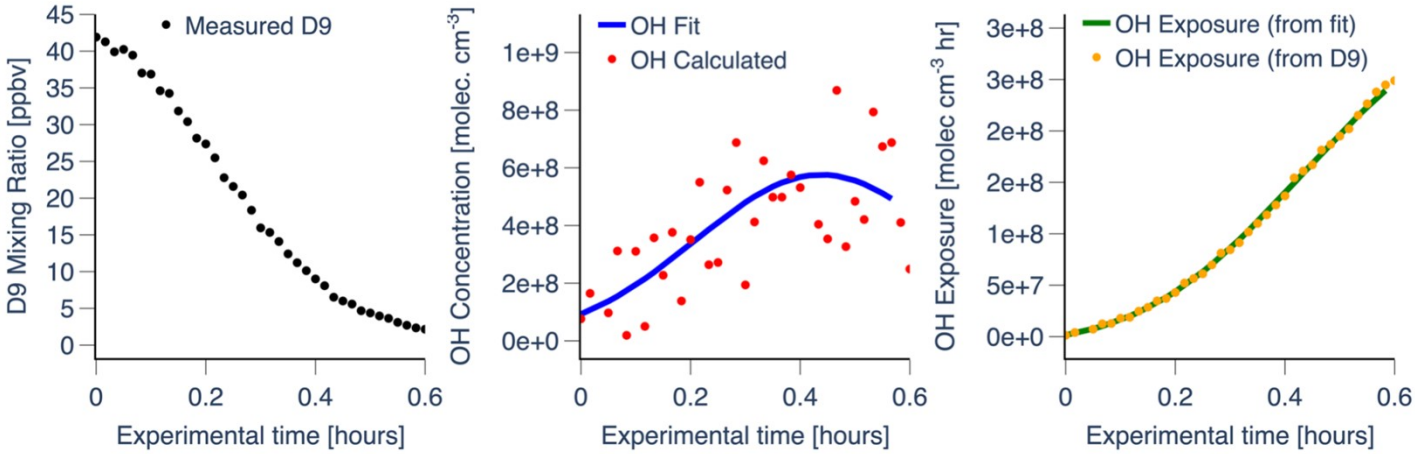

Figure S5: (a) Dilution-corrected mixing ratios for deuterated butanol (D9). (b) OH concentrations estimated from D9 decay and the Gaussian fit to the data. (c) Raw and fit OH exposure. All data are from the chamber experiment performed on Ponderosa Pine emissions (Fire 38)

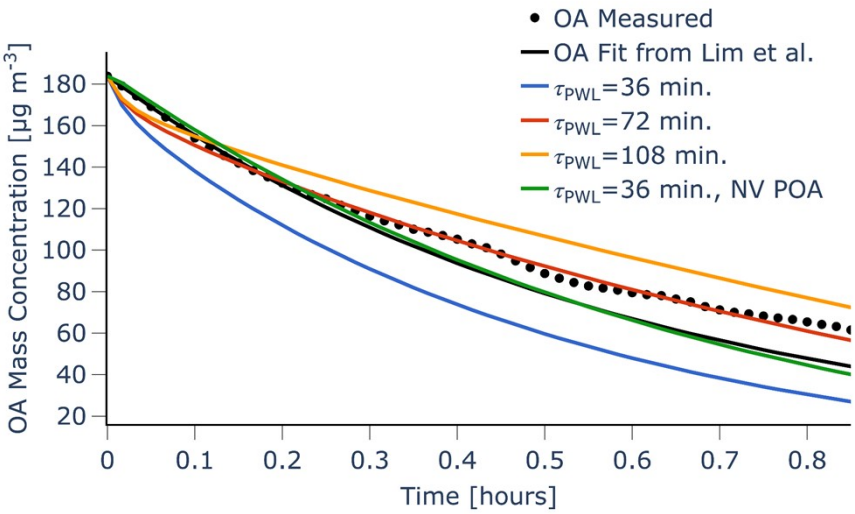

Figure S6: Dilution-corrected predictions of OA mass concentrations compared against measurements for different particle wall loss rates (τ of 36, 72, and 108 minutes) and assumptions about POA (semi-volatile versus non-volatile). Also shown is the particle wall loss rate estimated in Lim et al.[1] Model predictions and measurements are from a 'dark' experiment performed on a Ponderosa Pine Fire.

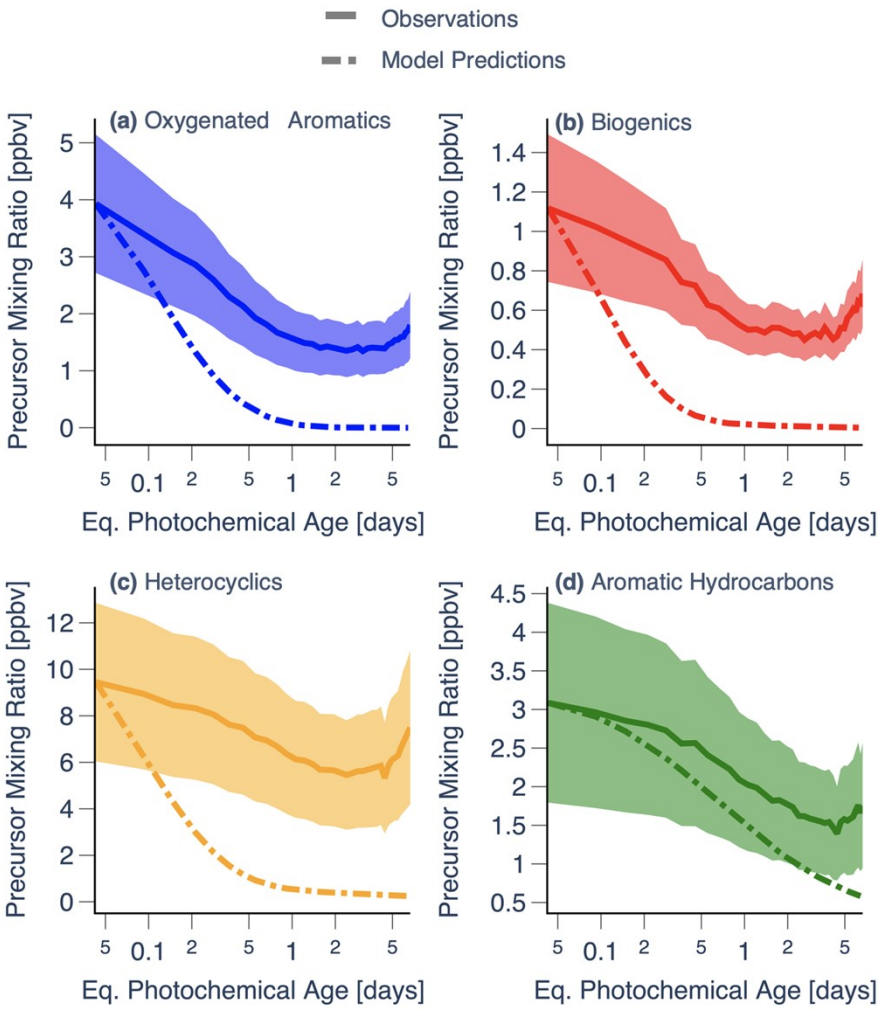

Figure S7: Model predictions of dilution-corrected SOA precursor mixing ratios compared against measurements and their uncertainties for the chamber experiment performed on Ponderosa Pine emissions (Fire 38). Individual SOA precursors were aggregated by the precursor class.

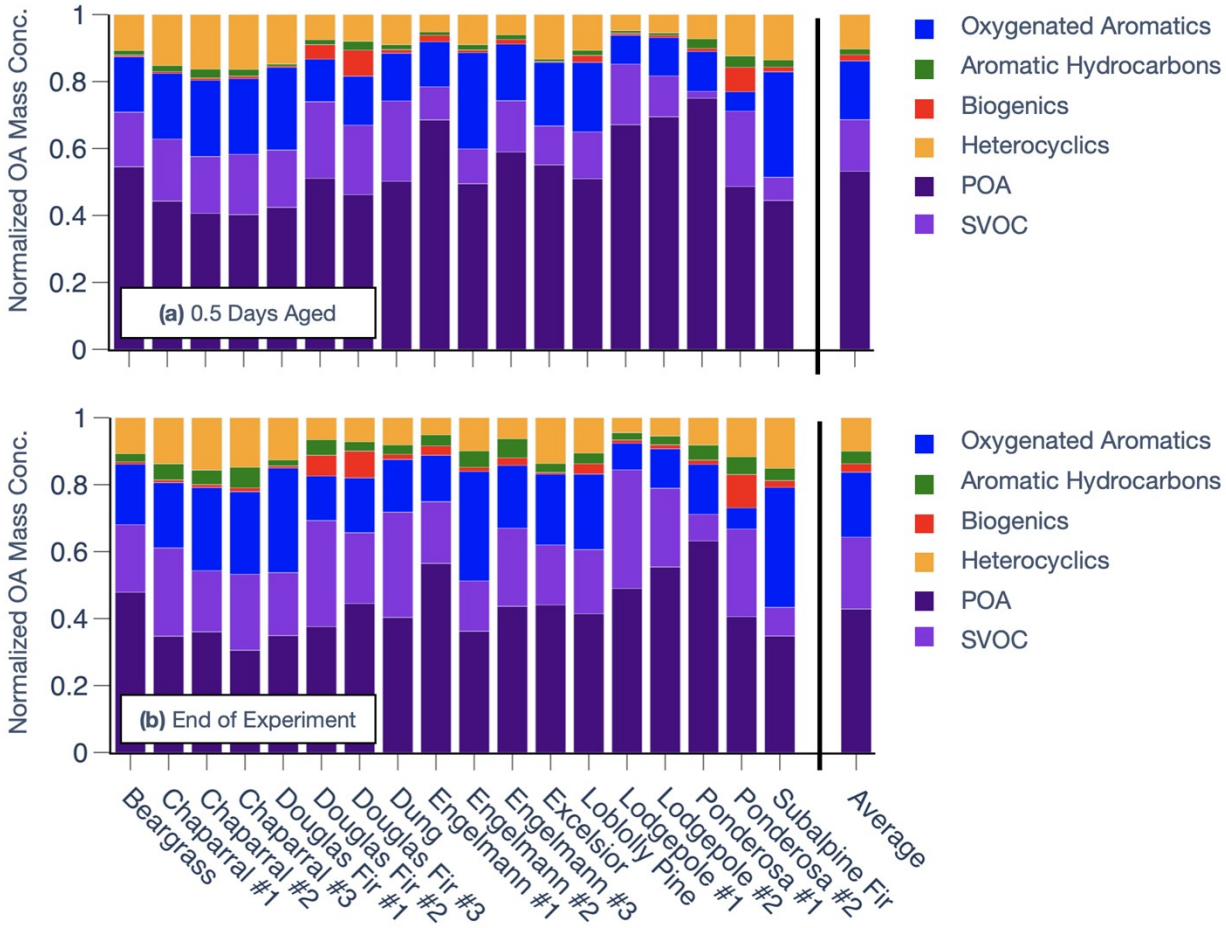

Figure S8: Model-predicted, normalized OA composition for all 18 chamber experiments as well as the arithmetic average. Composition includes POA and SOA resolved by precursor class. Results are presented at 0.5 equivalent days of photochemical aging and at the end of the experiment.

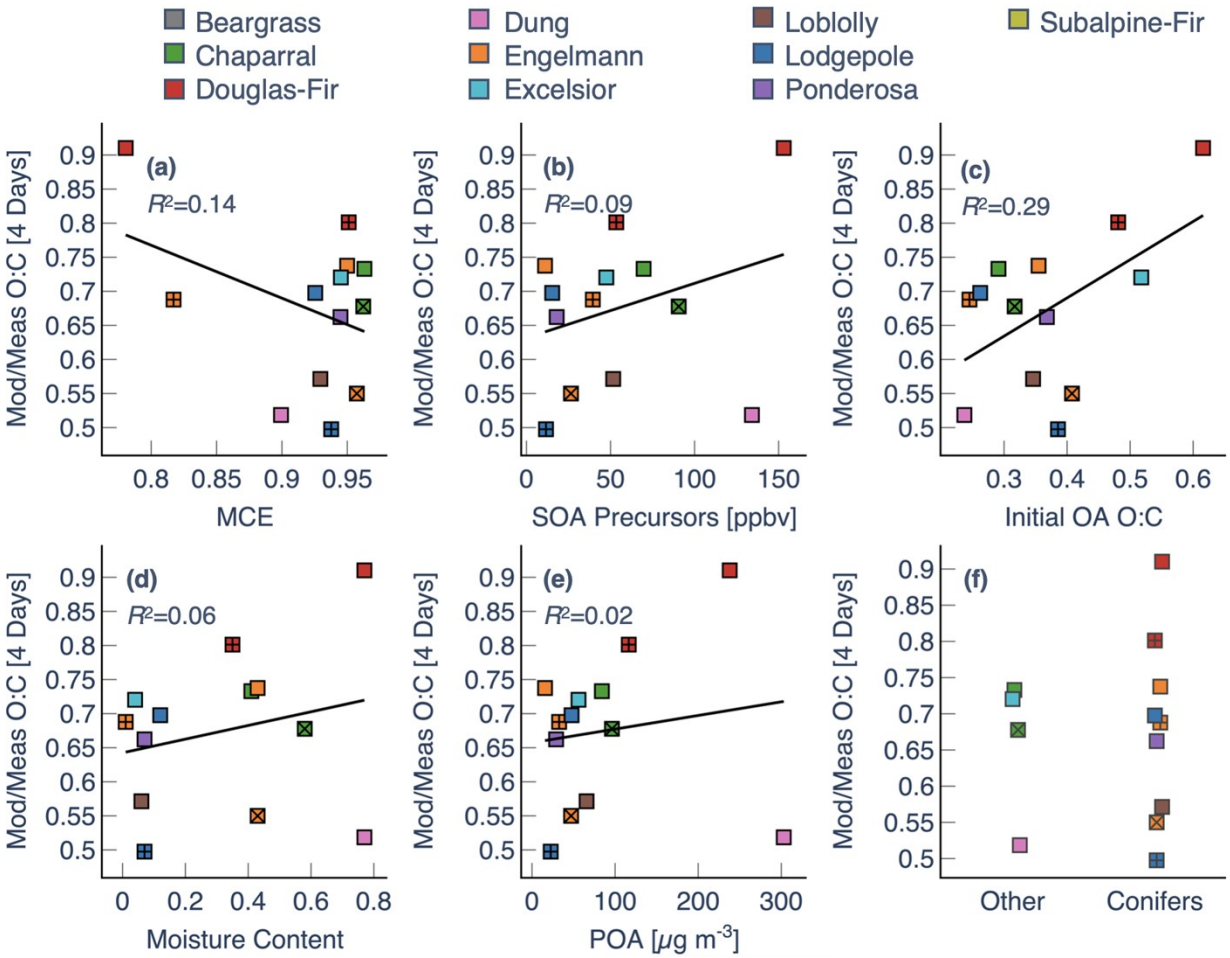

Figure S9: Model variance in OA mass expressed as a ratio of the modeled to measured OA compared against (a) MCE, (b) initial SOA precursors, (c) initial OA O:C, (d) fuel moisture content, (e) initial POA, and (f) fuel type (conifers versus others). Variance analysis is performed at a photochemical age of 4 equivalent days.

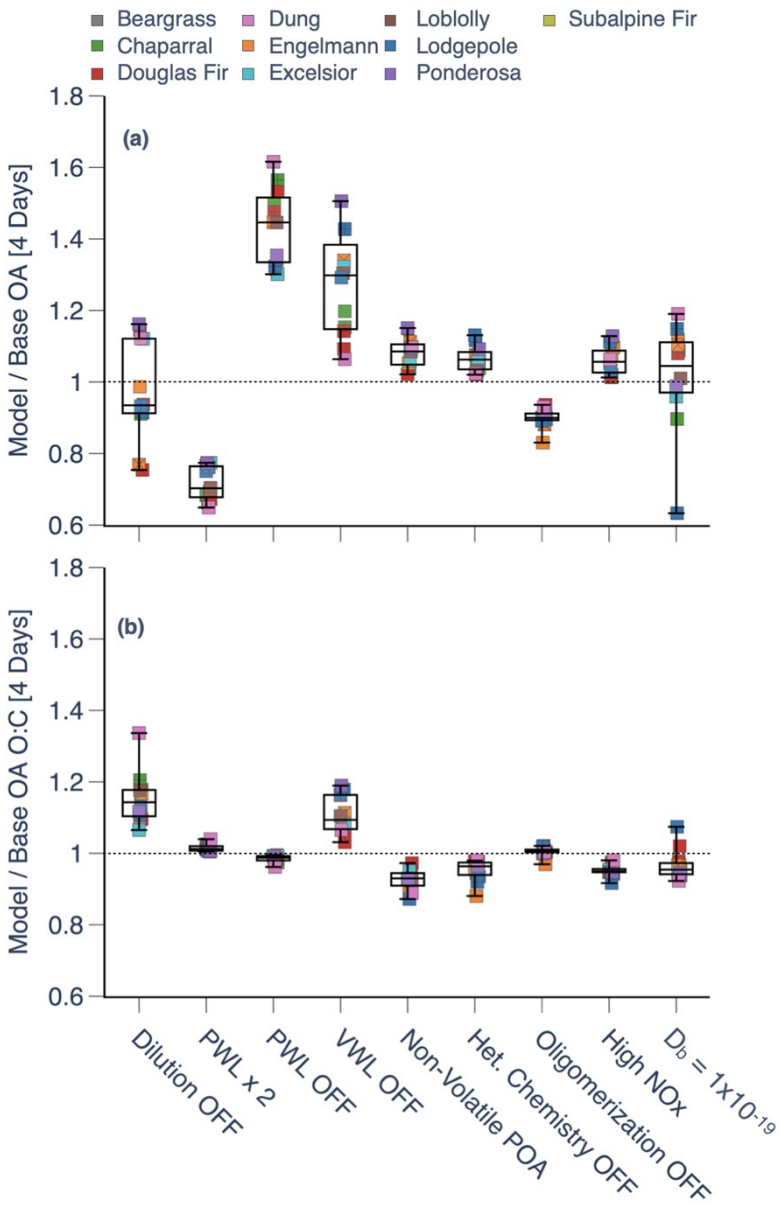

Figure S10: Model predictions from the sensitivity simulations ratioed to those from the Base simulation at four equivalent photochemical days for (a) OA mass concentrations and (b) OA O:C.

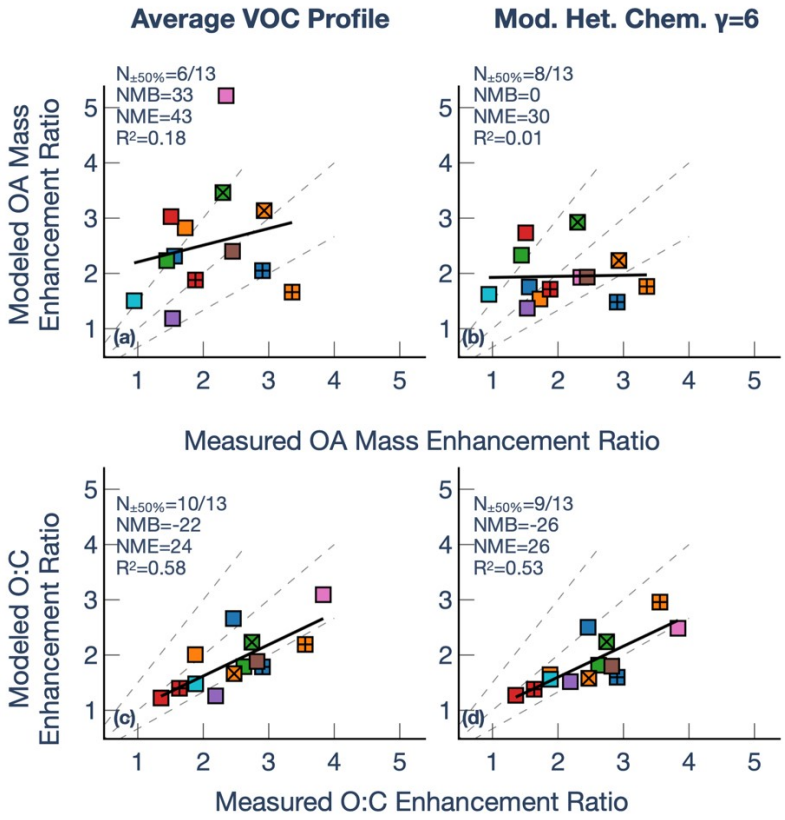

Figure S11: Same as the panels in Figure 4 but for two of the model adjustment schemes.

References

1 C. Y. Lim, D. H. Hagan, M. M. Coggon, A. R. Koss, K. Sekimoto, J. de Gouw, C. Warneke, C. D. Cappa and J. H. Kroll, *Atmos. Chem. Phys.*, 2019, **19**, 12797–12809.

2 A. Akherati, Y. He, M. M. Coggon, A. R. Koss, A. L. Hodshire, K. Sekimoto, C. Warneke, J. de Gouw, L. Yee, J. H. Seinfeld, T. B. Onasch, S. C. Herndon, W. B. Knighton, C. D. Cappa, M. J. Kleeman, C. Y. Lim, J. H. Kroll, J. R. Pierce and S. H. Jathar, *Environ. Sci. Technol.*, 2020, **54**, 8568–8579.

3 K. R. Bilsback, Y. He, C. D. Cappa, R. Y.-W. Chang, B. Croft, R. V. Martin, N. L. Ng, J. H. Seinfeld, J. R. Pierce and S. H. Jathar, *Environ. Sci. Technol.*, 2023, 57, 53–63.

4 N. L. Ng, J. H. Kroll, A. W. H. Chan, P. S. Chhabra, R. C. Flagan and J. H. Seinfeld, *Atmos. Chem. Phys.*, 2007, **7**, 3909–3922.

5 X. Zhang, C. D. Cappa, S. H. Jathar, R. C. McVay, J. J. Ensberg, M. J. Kleeman and J. H. Seinfeld, *Proc. Natl. Acad. Sci. U. S. A.*, 2014, **111**, 5802–5807.

6 P. S. Chhabra, N. L. Ng, M. R. Canagaratna, A. L. Corrigan, L. M. Russell, D. R. Worsnop, R. C. Flagan and J. H. Seinfeld, *Atmos. Chem. Phys.*, 2011, **11**, 8827–8845.

7 L. D. Yee, K. E. Kautzman, C. L. Loza, K. A. Schilling, M. M. Coggon, P. S. Chhabra, M. N. Chan, A. W. H. Chan, S. P. Hersey, J. D. Crounse and Others, *Atmos. Chem. Phys.*, 2013, **13**, 8019–8043.

8 Y. He, B. King, M. Pothier, L. Lewane, A. Akherati, J. Mattila, D. K. Farmer, R. L. McCormick, M. Thornton, J. R. Pierce, J. Volckens and S. H. Jathar, *Environ. Sci. Process. Impacts*, 2020, **22**, 1461–1474.